Conference on Future Automotive Technology

Focus Electromobility
München, March, 18-19th 2013

Simulating low temperature behavior of high voltage traction batteries – The challenge of real time efficiency estimation

Johannes Lieb[1], Fabian Czuppa[1], Stefan Knoll[1], Jochen Schröder[1], Bernard Bäker[2]
[1]*BMW Group, Munich, Germany*
[2]*Institute of Automotive Mechatronics, IAM GmbH, Dresden, Germany*
E-mail: Johannes.Lieb@bmw.de

ABSTRACT:

The efficiency of the traction battery is directly linked to an electric vehicle's performance and driving range. Real time efficiency estimation during driving as well as offline simulation is dependent on the use of battery models. The challenge of simulating battery behavior lies in its nonlinearity, which is particularly apparent at low cell temperatures. This paper presents an equivalent circuit model that is parameterized and validated at a wide temperature range between -20°C and +24°C. A pragmatic approach is introduced that allows incremental fitting of the model parameters as well as the validation of intermediate simulation steps. The resulting parameters show a high dependence on temperature, indicating that this degree of freedom needs to be given in the modeling process to achieve good results at varying temperatures.

Keywords: Lithium ion, equivalent circuit model, low temperatures, electric vehicle

1 INTRODUCTION

In recent years, the progressive increase in prices for fossil fuels as well as ambitious CO_2 emission policies have lead to a rising demand for more efficient vehicles. Electrification of the powertrain is a feasible way to ensure high energy efficiency and enable true emission-free driving. However, introducing this new technology to a market dominated by internal combustion engines also poses many challenges and possible risks for car manufacturers.
On the pursuit for optimal purpose designed electric road vehicles the BMW Group is systematically testing the latest technology under real world conditions. Since 2008, hundreds of drivers of the MINI E, a battery electric conversion from the MINI hatchback, have shared their experiences in dealing with driving range, their recharging habits and vehicle behavior at various environmental conditions. In 2011, an electrified version of the BMW 1Series coupé, the ActiveE, was released and given out to selected customers [1]. It is powered by the first complete set of in-house drivetrain components, meaning that the traction e-machine as well as the inverter and the high voltage battery system were developed at BMW. As a further development they will form the electric powertrain of the i3, the first purpose designed battery electric megacity vehicle. It will be released in 2013 and benefit from the insights gained from the intensive real world deployment of the electric drive system. As an example the work presented here is based on the hv-traction battery of the ActiveE.

Lithium ion based storage systems are currently the most promising technology for vehicular application, but to date energy storage is still the limiting factor to electric mobility due to their relatively low specific energy density and high costs [1]. Further development is needed to increase storage capacity and economic viability of high voltage traction batteries while maintaining a high level of safety, reliability and durability. In contrast to the still prevailing combustion engine powered cars the electric vehicle's driving performance and energy efficiency are greatly influenced by the current condition of its energy source. Therefore modern battery management systems (BMS) continuously monitor the behavior of the single cells to derive the system's state of charge (SOC) as well as to predict its future capability to deliver and receive electric power, often referred to as state of function (SOF) [2–4]. As this work intends to demonstrate, the battery's efficiency is directly linked to the dynamic voltage behavior during operation. Battery performance and efficiency are in turn related in two ways: The cell voltage needs to be restricted to a certain operating range. Depending on the current state, the battery's power ability may need to be reduced in order to abide the voltage limits. As a secondary effect, to provide constant power the current needs to increase as the voltage drops during load. This may lead to performance degradation based on the given current operation limits. As already mentioned the BMS needs to monitor, as well as predict the battery's performance and efficiency respectively to provide safe and reliable operation. The challenge is that the battery's dynamic behavior is highly nonlinear and is strongly depending on system parameters like temperature and SOC as well as the battery's recent history of stress. Therefore, dynamic battery models are usually implemented on board the vehicle. In the context of efficiency estimation, the battery model can fulfill two functions:

– To determine the momentary efficiency, the battery model complements the measured current and voltage information by necessary system parameters like the SOC and idle voltage.
– For prediction algorithms, e.g. estimating the remaining driving range, the battery model can be used to determine the future efficiency based on upcoming routes.

This work concentrates on offline vehicle simulations based on velocity profiles as it is equivalent to the second function listed above. Since vehicle simulations demand a defined power from the battery rather than a defined current flow, high model accuracy is vital to prevent model drift. The term *real time efficiency* is used to differentiate from other definitions of battery efficiency, usually representing the integral *energy storage efficiency*.
For this type of application, impedance-based battery models are most common (cf. [2], [3], [5–8]). One established method is to use electrical equivalent circuit models (ECM) to reproduce the battery's current and voltage behavior by means of lumped elements. It has the necessary degrees of freedom to represent a good compromise between computational effort and achievable accuracy for the given task. The choice of elements and modeled dependencies determine the complexity and the necessary parameterization effort. There are quite a few publications that highlight fast and practicable parameter determination, e.g. [3], [7], [8]. However, applicability of the presented methods on a wide temperature range is usually not presented or is listed as future work. Especially at low temperatures, battery behavior is known to change significantly, affecting the previously described characteristics efficiency and performance. Furthermore, the individual partial reactions forming the macroscopic clamp behavior can be expected to change differently making the use of simplified models more challenging. Temperature dependency is usually analyzed using thermodynamic models (cf. [9–12]), normally in combination with cell-based measurements at various temperatures.

This paper concentrates on the change of the equivalent circuit model parameters at low temperatures and the achievable accuracy with the model presented. The aim of this work was to develop a pragmatic approach for parameter determination and validation using various measurement profiles. By following the incremental method applied here it is also possible to examine intermediate states of the model and incrementally improve the models accuracy.

2 LI-ION BATTERIES AT LOW TEMPERATURES

Figure 1: Low temperature dynometer measurements at BMW energetic test facility

2.1 Theoretical background

It is vital to understand that the electric behavior observed at the battery clamps is the result of a series of electrical, chemical and electrochemical processes that take place simultaneously within every cell of the battery. The authors of [9] distinguish between a total of seven relevant partial processes, that each have a different contribution to the current voltage behavior of the cell. They represent the ohmic behavior of the two electrodes and the electrolyte, partial voltages caused by concentration gradients in the electrodes and electrolyte as well as charge transfer processes at the electrodes. Other categorizations can be found in literature depending on the specific research question but it is reasonable that the absolute impact of low temperatures can vary for the different partial reactions.

As one general tendency, the reaction rate of a chemical process decreases exponentially towards lower temperatures, a phenomenon described by the *Arrhenius equation* [13]. Because of its simplicity it is often used in the context of battery modeling. According to [12], [14] the impact of ion conductivity in the electrolyte based on diffusion shows Arrhenius type behavior. The detailed breakdown of partial effects in [9] shows that diffusion processes have the longest time delays on discharge pulses. They result from concentration gradients in the electrolyte and active material. At low temperatures there are higher time constants and larger amplitudes to be expected in the voltage responses due to diffusion retardation. Another fundamental equation in the context of electrochemistry is the *Butler-Volmer equation*, which also includes an exponential dependency on temperature. It describes the dependency between the electrode current and the necessary overpotential to drive the charge transfer process, e.g. during Li+ insertion and extraction. By putting the overpotential and current in relation, an empiric resistance can be calculated. As a typical Butler-Volmer characteristic the calculated resistance also depends on the current itself, resulting in higher values for low magnitudes of currents. Towards low temperatures this nonlinear effect is even intensified. When this effect dominates over mass transport related effects, the battery will show comparably high voltage drops at low temperatures under low stress.

2.2 Observations based on measurement data

In the course of the research project EFA2014/2 [15], an extensive measurement campaign has been conducted to evaluate the energetic impact of low temperatures on a battery electric vehicle. The BMW ActiveE [1] was used as reference vehicle. Its battery system is comprised of 192 SBLimotive 40Ah cells connected as 96 pairs in series. The cathode material is commonly referred to as *NMC* (Lithium Nickel Manganese Cobalt Oxide). The drive cycle measurements were carried out at several temperatures between -20°C and +24°C. To obtain comparable and realistic driving situations the FTP-72 cycle (see Figure 3) was used for all temperatures. Before each measurement the entire vehicle including the hv-traction battery was preconditioned to the corresponding environment temperature at the BMW climate chamber (cf. Figure 1). This created a valuable selection of measurement data for examining real life battery behavior as well as means to develop a realistic battery model. The measured data from the vehicle tests were afterwards scaled down to cell level for the parameterization process. In addition to the vehicle measurements there were also constant current pulse relaxation measurements of single cells available at different temperatures and a current rate of C/3. This allowed observing the clamp behavior at different temperatures without a dynamic change of current flow.

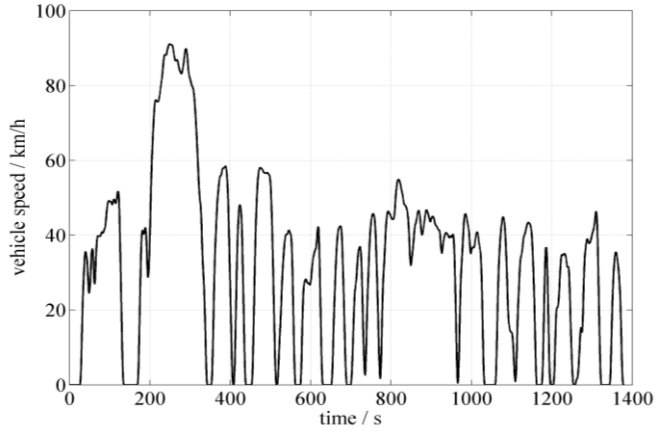

Figure 3: US FTP-72 driving cycle [16]

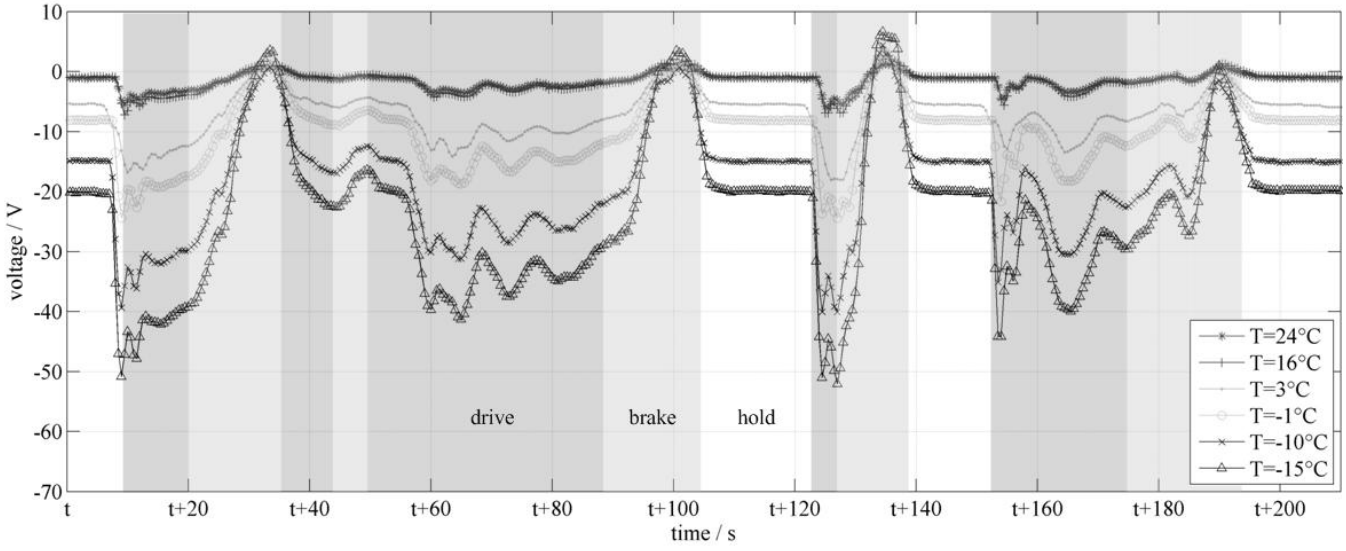

Figure 2: Voltage difference relative to idle voltage of the battery system during a selected period of FTP-72 drive cycle

Figure 2 shows the battery's dynamic voltage during a representative selection of 200s of driving the FTP-72 cycle. For better comparability the idle voltage (see Chapter 3.1) has been subtracted from the measured clamp voltage. The SOC of the individual measurements were in a range of 80% - 90% so that this step seems eligible.

– The most obvious change in behavior at low temperatures is the much higher amplitude of voltage response in comparison to the measurement taken at +24°C. The power demand of the vehicle was almost identical in the depicted situation.
– In this selection the lower voltage limit was never reached but it is quite apparent that discharging performance can be limited at low temperatures and lower SOC due to the high voltage drops.
– During standstill the voltage drop caused only by the climate system and 12V-bordnet is disproportionally high at low temperatures. The climate control system was always activated and except for the +24°C measurement it had the same electric power demand.

As previously mentioned, the partial reactions within the cell can take place at different rates. The dynamic clamp voltage therefore also depends on the recent history of stress. In the drive cycle measurements this time dependency is not clearly visible because of the current changing dynamically. To observe influence of time on the clamp voltage, constant current pulses are beneficial. They are usually taken on cell level, but with identical cells this behavior can be scaled to the entire battery system. Figure 4 shows the clamp voltage progression at three selected temperatures to display the change of behavior. The current pulses of approximately C/3 were held constant until 10% SOC was depleted. For the +25°C measurement 5% increments were used.

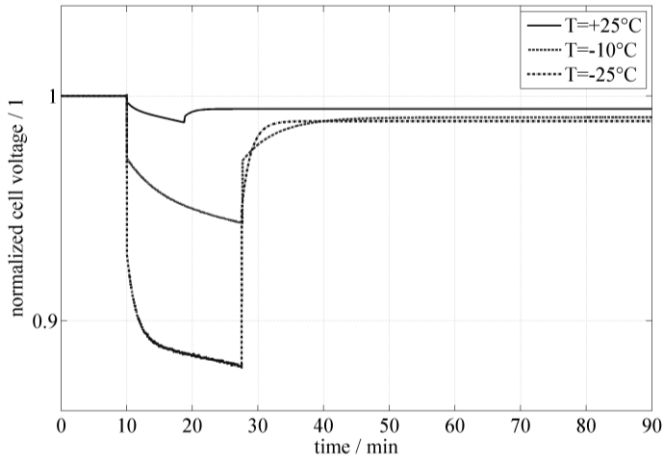

Figure 4: Voltage response to C/3 current pulses at different cell temperatures

In Figure 4 the following observations can be made:

– There is an initial voltage drop upon surge current which increases at low temperatures.
– After a certain time the voltage plot is approximately linear.
– At lower temperatures it takes longer until this steady state is reached in the voltage progression.
– After taking back the surge current at t = 28 minutes there is an initial voltage step, followed by a relaxation phase.
– The relaxation time until a constant voltage is reached increases at low temperatures. Note that the idle voltage of the +25°C measurement is higher since only 5% SOC are drawn.

The current pulse measurements indicate that there are reactions that happen instantaneous within the regarded time scope. Other partial reactions seem to have a distinct time-dependent behavior. The approximately linear change of voltage upon surge can be explained by the linear decrease of SOC and the correlating idle voltage[1]. The difference between the instantaneous reaction and the voltage drop at steady state can be described as a time-dependent increase of the cell's internal resistance. Overall, low temperatures seem to influence both the instantaneous and the time-dependent reactions upon surge current and relaxation. Since the measurements were taken at one current level only, possible impact of current variation could not be examined.

3 BATTERY MODEL DEVELOPMENT

3.1 Model selection

In the course of this work an equivalent circuit model (ECS) capable of real time efficiency estimation and prediction at a wide temperature range shall be developed. As previously mentioned, the ECS mimics the battery's clamp behavior by rebuilding the relevant partial reactions by means of partial voltages over lumped-elements (e.g. resistors, capacitances or inductances). For this work a series arrangement of voltage source, ohmic resistance and one RC-couple was chosen (cf. Figure 6). The selection of elements including their modeled dependencies defines the degrees of freedom for the created model and therefore the number of individual phenomena that can be distinguished. Obviously a compromise between accuracy and parameterization effort has to be made. Based on the observations (cf. chapter 2.2) the model needs to incorporate at least three elements representing time dependant and instantaneous reactions (approximately time-independent) as well as the SOC progression. Figure 5 classifies some of the dynamic effects already mentioned according to their typical time ranges. For driving a battery electric vehicle the relevant time range is between tenth of seconds (dynamic filtering within drivetrain) and several hours (electric driving range). Reactions that happen faster can therefore be assigned pure ohmic behavior without sacrificing too much accuracy. Slower reactions like ageing are not considered in this work. Also, effects that are caused by inhomogeneous distribution of the system's total resistance and capacity over the cells cannot be simulated with this model. This is because the battery system is modeled as the combination of 192 identical cells to reduce computational effort.

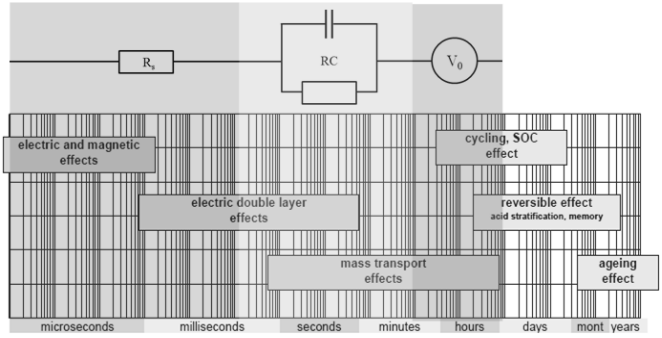

Figure 5: Typical time ranges of different dynamic effects [17] including an approximation of the corresponding ECS element

Because of the selected model most elements will cover multiple effects as depicted in Table 1. It should be noted that only a rough classification is possible since the absolute impact of each partial reaction cannot be fully allocated in the equivalent circuit model. As one objective of this work is to display the impact of temperature on the model parameters the corresponding dependency was given for all elements. Figure 5 suggests how the selected elements cover the various dynamic reactions.

Table 1: Allocation of battery reactions to lumped elements

Element	Dependency	Modeled effect
R_s	Current Temperature	Electric effects, Butler-Volmer behavior, mass transport (partially)
RC	Temperature	Concentration induced overvoltages, double layer effect (partially)
V_0	SOC Temperature	Empirical idle voltage after several hours ("down-curve", no hysteresis)

[1] Note that the idle voltage is usually nonlinear at very high or low SOC so that this approximation is not valid

The thermal behavior of the single cells is modeled rudimentary based on estimation of the cells heat capacity, without any spatial resolution. Ohmic losses (cf. equation (2)) represent the only heat flow. The reversible effect due to entropy change during charging and discharging is neglected. Comparison of simulation results and measurement has shown acceptable agreement. Also the temperature progression while driving the FTP72 cycle is quite small so that this simple approach is adequate.

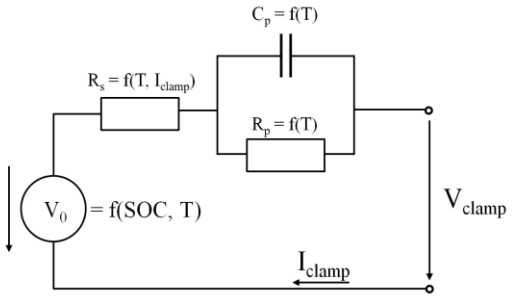

Figure 6: Equivalent circuit model incl. modeled dependencies

3.2 Energy conversion efficiency

The following chapter derives the relationship between the battery's efficiency and the clamp behavior and how it can be determined using the battery model. Depending on the individual scope of a research or application there are many definitions of battery efficiency to be found. Most definitions contain discharging as well as charging to determine the integral efficiency of the battery. One method is to measure the energy delivered by the battery during driving and divide it by the amount of energy needed to fully recharge it afterwards. This procedure is often sufficient, e.g. for well-to-wheel analysis but it does not give any information about the real time efficiency in a specific driving situation. Also, since charging is included, it is not possible to distinguish power losses occurring during driving only. This definition of efficiency is best described as *energy storage efficiency*. For the purpose of real time determination, however, the term *energy conversion efficiency* seems better suited. It relates the amount of chemical energy within the battery and the electrical energy at the clamps and can be calculated for charging and discharging individually. Note that empirical formulas like the *Peukert equation* are mostly not suitable for lithium-ion traction batteries since the prerequisite of quasi-stationary load is usually not given for powertrain application.

Lithium-ion batteries are known to have a coulomb efficiency very close to 100% during operation, meaning that no charge is lost in the energy conversion process. It only decreases during long-term degradation caused by calendaric aging or parasitic side reactions. Therefore, the short-term energy conversion efficiency can only be influenced by the clamp voltage. From a phenomenological point of view the negative impact of a voltage drop during discharge can be described in two ways:

- As the clamp voltage drops during discharge, the usable electrical energy decreases for a given decrement of SOC.
- As the clamp voltage drops during discharge, the clamp current thus needs to increase to obtain the same usable electric energy, leading to a higher decrement of SOC.

These two views are energetically not identical since they use a different value as a reference. The first one uses a predefined current profile whereas the second is based on a defined demand for electrical power. Current-based measurements and simulations are most common in the domain of battery research. However, the battery's behavior as a part of the electric drivetrain can only be represented correctly by power-based simulations. This is because the vehicle's operating strategy demands a defined power value from the battery to create a reproducible driving behavior. The power-based approach is especially important when investigating the effects of low temperatures in a vehicular application. Using identical current profiles for different temperatures would lead to incorrect SOC progression and cause the simulation to drift from the real behavior.

In the following section the energy conversion efficiency for charging and discharging shall be derived based on ohmic loss power. In general, the momentary energy conversion efficiency is defined as the ratio of usable power and power spent:

$$\eta_{conversion} = \frac{P_{usable}}{P_{spent}} \tag{1}$$

Due to power losses in the system caused by the ohmic losses, P_{usable} will always be smaller than P_{spent}. During simulation the loss power can be calculated from the resistances of the battery model:

$$P_{loss,sim.} = R_s \cdot I_{clamp}^{\ 2} + R_P \cdot I_{Rp}^{\ 2} \tag{2}$$

For any point in time an equivalent internal resistance $R_{equivalent}$ can be calculated from equation (2) or during measurement. Equation (3) shows that by applying *Kirchhoff's circuit laws* to this simplified battery model, the loss power can be determined by the voltage drop and the clamp current directly.

$$P_{loss} = R_{\text{equivalent}} \cdot I_{clamp}^{\ 2} = \left|V_{clamp} - V_0\right| \cdot I_{clamp} = \Delta V \cdot I_{clamp} \tag{3}$$

To calculate the energy conversion efficiency from the loss power and clamp power ($V_{clamp} \cdot I_{clamp}$) one needs to distinguish between charging and discharging since P_{usable} and P_{spent} are assigned differently. In the case of discharging the clamp power represents the usable power whereas during charging it represents the power spent. A path dependent evaluation of equation (1) results in:

$$\eta_{discharge} = \frac{P_{clamp}}{P_{clamp}+P_{loss}} = \frac{V_{clamp} \cdot I_{clamp}}{V_{clamp} \cdot I_{clamp} + \Delta V \cdot I_{clamp}} = \frac{1}{1+\frac{\Delta V}{V_{clamp}}} = \frac{V_{clamp}}{V_0} \tag{4}$$

$$\eta_{charge} = \frac{P_{clamp}-P_{loss}}{P_{clamp}} = \frac{V_{clamp} \cdot I_{clamp} - \Delta V \cdot I_{clamp}}{V_{clamp} \cdot I_{clamp}} = 1 - \frac{\Delta V}{V_{clamp}} = \frac{V_0}{V_{clamp}} \tag{5}$$

It shows that the momentary efficiency can be expressed by the ratio between the measured clamp voltage and the battery's idle voltage. This ratio is in general referred to as *voltage efficiency* of a galvanic (discharging) or electrolytic (charging) cell. As long as the coulomb efficiency can be approximated by 1 it is equivalent to the *energy conversion efficiency*. The initial motivation for using a battery model was to estimate the energy efficiency in the current situation as well as for vehicle simulations. As equation (4) and (5) demonstrate, the calculation is very simple but there is at least one necessary parameter that can't be measured during operation. As a first order approximation the idle voltage could be low-pass-filtered from the measured clamp voltage but especially at low temperatures this estimation would be unreliable due to the time-dependent reactions. A common method is to use *Kalman-Filtering* to estimate the necessary parameters online (see [2], [6], [18]). For that a complete battery model is needed, likewise for offline simulations. The following chapter will present how the model parameters for this work were obtained.

3.3 Parameterization approach

The novel approach of this paper is to separate the time-dependent parts of the model from the time-independent (within the time scope of EV operation) parts and parameterize the model incrementally. All partial reactions that are affected by the recent history of stress within the relevant time scope (cf. chapter 3.1) are considered time-dependent in contrast to reactions modeled by pure ohmic behavior. By dividing the model into those two categories they can be parameterized separately which enables individual choice of the best fitting method for the given parameter. It may, for example, be beneficial to use a different optimizing algorithm for the RC parameter than for the R_s parameter.

Kirchhoff's voltage law applied to the equivalent circuit model (cf. Figure 6) shows how the clamp voltage is modeled as a superposition of the partial voltages:

$$V_{clamp} = V_0 + V_{Rs} + V_{RC} \tag{6}$$

Figure 7 visualizes the partial voltages of equation (6) during a selection of the FTP-72 driving profile.

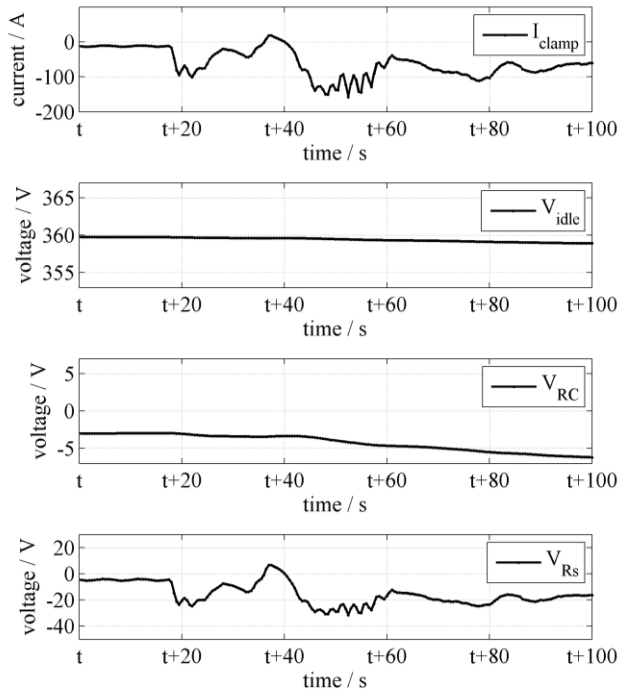

Figure 7: Visualization of the partial voltages of the model during a defined current profile

For the parameterization process it is essential to use current-based input profiles for the simulation. Since the current flow through every element is fixed, the three partial voltages do not interact with each other and their behavior can be examined separately. If the parameters are modeled with a SOC dependency, of course, this needs to be taken into account. Since the change of SOC usually has a large time constant it can be considered constant for a short period of time. For this work the measurements did not exhibit a strong dependence on SOC, especially in the region between 20% and 80%. For further improvement, using a fitting algorithm with the SOC as an additional degree of freedom could be considered.

As a first step the less dynamic but time-dependent parameters idle voltage and RC-couple are parameterized. The idle voltage is modeled as a lookup table of cell voltage over SOC. To acquire the needed voltage steps defined charge portions of 10% SOC were taken subsequently from a fully charged single cell followed by several hours of relaxation time. The voltage level right before the next current pulse was then used for the lookup table. Repeating this procedure at different temperatures resulted in a total of four look up tables. The SOC progression within the simulation is calculated by means of standard *coulomb counting*, meaning that the SOC is determined solely by the integral of the cell current in relation to the nominal capacity of the cell (C_{nom}). A coulomb efficiency of 100% is assumed.

$$SOC(t) = SOC_{t_0} + \frac{1}{C_{nom}} \cdot \int_{t_0}^{t} I_{clamp}(t)dt \tag{7}$$

The measurement profiles used for the idle voltage curves are then also used to determine the parameters of the RC-couple on cell level. During the constant current pulses used for the idle voltage determination, the time-dependent behavior is clearly visible for the different temperatures (cf. Figure 4). Since only one RC-couple is used in this work, a graphic method for parameterization could be chosen (cf. Figure 8). By subtracting the initial voltage drop caused by R_s and the linear change of idle voltage during the constant current flow, the effect of the RC-couple can be retrieved. Figure 8 shows how the curve is fitted determining the R_p and the time constant τ under load. As previously mentioned, no SOC dependency was modeled. Also, the RC-couple was fitted at one current level of C/3 only.

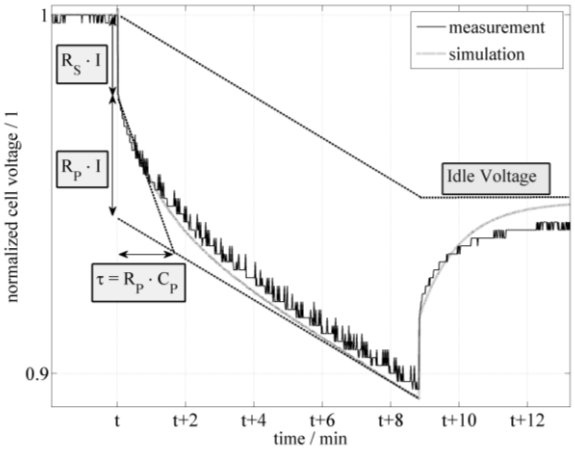

Figure 8: Graphic determination of RC-parameters at one exemplary temperature

In the second step the parameter map for R_s depending on temperature and current (cf. Table 1) is created. The fitting method applied here is based on the theory that the pure ohmic behavior of R_S (cf. Figure 7, bottom graph) can be directly calculated from the clamp voltage and current once the time-dependent partial voltages have been determined. To do so, any dynamic current profile can be used as input to the intermediate simulation environment, containing only the idle voltage determination and the RC-couple. Preferably a profile close to the real vehicle application is used, covering all relevant load scenarios. For this work the FTP-72 vehicle measurements at the various temperatures were used to parameterize R_s and to validate this method. Since the measurements contain the clamp voltage and current of the entire traction battery system, the voltage drop was scaled to cell level, thus representing the median cell resistance. With the time-dependent part subtracted, R_s is determined by:

$$R_S = \frac{V_{clamp} - V_0 - V_{RC}}{I_{clamp}} = \frac{V_{Rs}}{I_{clamp}} \tag{8}$$

Equation (8) can be evaluated for entire cycle measurements or at distinctive points (e.g. current peaks) throughout a dynamic measurement. For this work, the latter method was used to gain experience in the sensitivity of the model parameters. Missing sample points were added by graphic interpolation. When using entire measurement arrays some filtering of the resulting resistance map may be necessary. Especially at very low current values the sensitivity towards model deviations is high, resulting in scattered resistance values. Here an average value can be used. Note that the resistance value at zero Ampere is merely a numeric measure and has no real physical justification.

3.4 Validation techniques

The quality of a model can be determined in several ways, also because the definition of the term *quality* itself is variable. It depends on what specific purpose the model is supposed to fulfill. Long-term charging simulations require a different kind of accuracy than, e.g. high power performance simulations. To quantify the validity of the simulation usually reference profiles are used to determine the deviation between simulation and real cell behavior. The challenge is that only the resulting clamp behavior of the cell can be compared with the model, whereas intermediate parameters like the idle voltage or allocation of partial overvoltages can't be measured directly

during operation. By choosing the right methods, however, even the integral clamp behavior of the real cell can give an indication of quality for certain subparts of the model. The following paragraphs give an overview of different validation techniques and which group of model parameters they aim at.

Current profiles that cover a wide range of SOC are well suited to test the idle voltage determination of the model. After a sufficient relaxation phase, the clamp voltage can be compared with the idle voltage calculated by the simulation. During load only the qualitative progression of V_0 can observed, since other time-dependent reactions also contribute to the clamp voltage. Due to the fixed current profile the SOC determination is not influenced by deviations of the resistance parameters and can therefore be examined separately. This kind of profile, however, should not be chosen if the model is to be used for efficiency analysis. The integral accuracy of the battery model as it would behave in a vehicle simulation can only be tested if power-based profiles are used as reference profile. As previously mentioned this checks the interaction of all components, since any deviation of voltage leads to a deviation of current flow and therefore has an effect on the SOC progression. Long-term simulations like charging analysis are especially fault prone because SOC drifting will lead to a change in charging time. Power-based load profiles are more difficult to control in the laboratory, but for testing the integrity of the model it is valid to calculate the clamp power profile from a current-based measurement. The deviation between the two simulations will give further indication of the validity of the model.

The precision of the ohmic part of the model can be checked at any current step within a measurement (cf. Figure 8) or also during operation of the vehicle. A rapid change of the current flow is essential to observe the reaction without the voltage change caused by the RC-couple or the idle voltage.

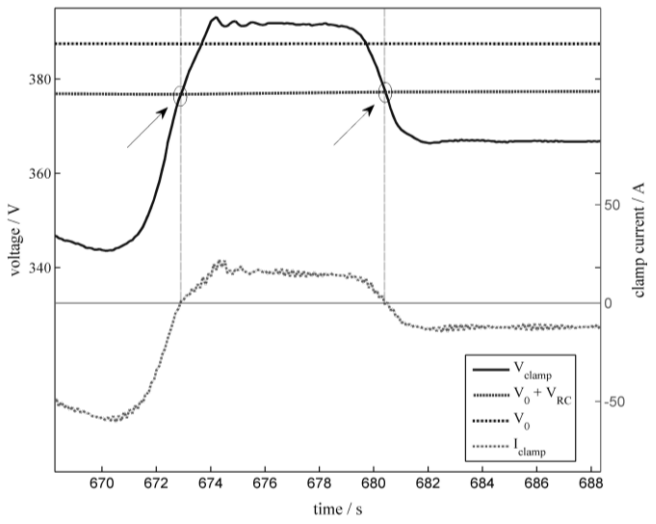

Figure 9: Validation method based on voltage sum at zero crossing

The quality of the RC-couple in representing the time-dependent reactions can be checked in several ways. One is measuring the clamp voltage in long-term constant current pulses and relaxation phases as depicted later in Figure 12. Since the change of idle voltage needs to be subtracted in those measurements, it is vital to validate the idle voltage determination algorithm first. Another indication that the time-dependent reactions are represented correctly can be obtained during the parameterization phase itself. Since the ohmic part of the model should be determined last (cf. equation (8)), a drift of V_0 or V_{RC} would result in widely scattered values for R_S at identical current and temperature values. So being able to fit R_S according to the given dependencies current, temperature and SOC (not applied) confirms the validity of the previous modeling steps.

Current profiles that include charging as well as discharging phases include a similar indication of quality of the time-dependent components. This validation method is based on the theory that at the point of zero crossing of the clamp current, the overvoltage caused by R_S disappears, simplifying equation (6) to:

$$V_{clamp} = V_0 + V_{RC} \tag{9}$$

Any time the current measures zero, e.g. when engaging regenerative braking, the time-dependent partial voltages can be rechecked. If the sum of idle voltage and voltage drop caused by RC is not equal to the clamp voltage at zero crossing, then the combination of V_0 and V_{RC} has drifted. Since the idle voltage can be checked separately, this can be a valuable indication for the validity of the RC-couple at any given point in time during a load profile. Figure 9 visualizes this approach at an example of two current zero crossings. Without considering the voltage drop over the RC-couple, the points in times at which the current crosses zero and the voltage crosses the idle voltage would not match.

4 RESULTS & DISCUSSION

4.1 Temperature dependency of model parameters

The result of the parameterization process of R_S is shown in Figure 10. *Butler-Volmer behavior* (cf. chapter 2.1) is clearly visible: the calculated resistance value representing the necessary overpotential for the current flow increases for low current values. This effect is less distinct at +25°C but much amplified at low temperatures. At -20°C and a current value of approximately 10A the resistance measures 25 times the value at +25°C. This phenomenon is in accordance with the observed behavior in Figure 2 where the voltage drop during vehicle standstill is disproportionally high. For better visibility of this effect the change of resistance for four selected current rates is depicted in Figure 11 (bottom).

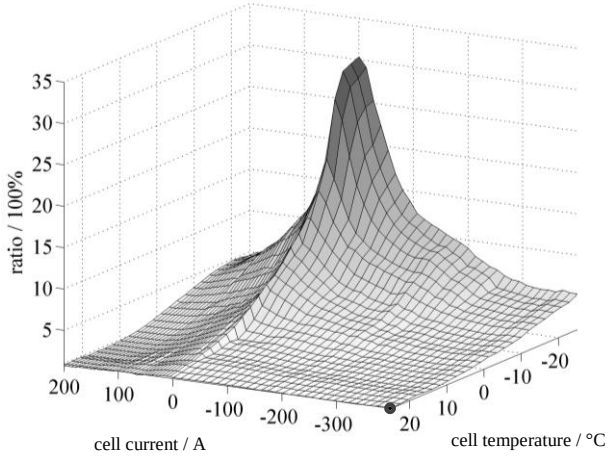

Figure 10: Parameter map of Rs plotted relative to value at -400A and +25°C

The progression of the RC parameters over temperature is shown in the top graph of Figure 11. It represents the result of the graphic parameterization step depicted in Figure 8 carried out at several different temperatures. As already visible in the current pulse reactions in Figure 4 the time constant as well as the resistance value increases at lower temperatures: The voltage drop caused by the time-dependent reactions increase in magnitude and it takes longer until a steady state is reached. The simulation results of three representative current pulses at different temperatures are shown in Figure 12. The results show that the behavior under load is represented much better than the relaxation behavior. This is particularly distinct at low temperatures but is also the case for the +25°C measurement. Additionally, also the fitting quality of the behavior under load decreases at lower temperatures. Since the shape of the voltage reaction seems to change it couldn't be fitted by the RC-couple. This indicates that the various time-dependent partial reactions within the cell must be affected differently by low temperatures. Other research papers, e.g. [3] and [7] suggest using more than one RC-couple to better represent the time-dependent behavior. The authors of [3] particularly highlight the improvement of simulated relaxation behavior using two RC-couples. However, it is not sure how relevant the modeling of relaxation is for dynamic drive cycle simulations.

Due to the constant current demand of the logical bordnet and the optional climate control there is no real relaxation during operation.

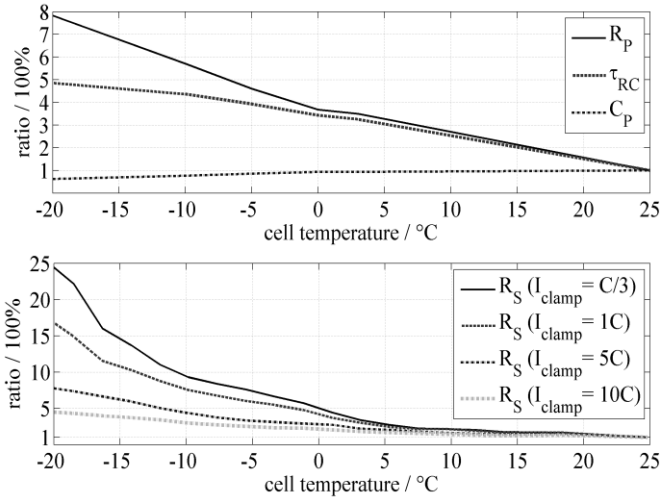

Figure 11: Change of model parameter values with temperature relative to +25°C

The idle voltage (not depicted here) did not show distinct temperature dependence. The remaining voltage difference after a six hour relaxation phase could be neglected compared to the other effects.

4.2 Achieved simulation accuracy in driving cycle

To assess the overall quality of a simulation model the rms (root mean square) value of the model deviation is commonly stated. Using the measured current profiles as input for the simulation the model deviation was determined by subtracting the simulated cell voltage from the measured clamp voltage. Figure 13 shows the achieved accuracy of the current-based simulation throughout the course of one FTP-72 cycle (~1400 seconds). As a general trend the absolute voltage error increases at low temperatures. It should be noted that the average amplitude of voltage reaction at -20°C measured about ten times the values at +24°C. Therefore, as a first order approximation, the relative error remains constant on the temperature scope analyzed. Figure 13 also includes the results of the respective power-based simulation. The power profiles were created by the measured clamp voltage and current. For the rms value at the highest temperature measured there is no deviation between the current and the power-based profile. Towards lower temperatures the deviation increases gradually, reaching its maximum at -20°C where the rms value for the power-based simulation is 6.7% higher. The reason for the higher difference at low temperature lies in the higher voltage amplitudes at the low temperatures: As mentioned before, the lower voltage forces a different operating point of current and voltage in the battery to match the demanded power. The resulting voltage of the simulation is in average lower than the current-based calculation shown before. The additional voltage error when using the power-based profiles could therefore be considered as a secondary effect of the model inaccuracies. It should be noted that these two types of simulations cannot be compared unambiguously by only looking at the voltages since the clamp current deviates as well. This comparison is merely given to draw attention to the fact that the stated model accuracy is also dependent on the type of simulation profile.

To give an overview of the voltage error distribution, Figure 14 contains histograms of four selected temperatures. As already the rms values suggest, the low temperature simulations also show highest absolute deviations. The distribution of the voltage error around zero indicates how well the median behavior is represented by the model. If for example the time-dependent parts were incorrect and caused the voltage level to drift this would show up as a biased voltage show up as a biased voltage error distribution towards one side. Looking at the distribution, it seems that the higher temperature that the higher temperature simulations in general have

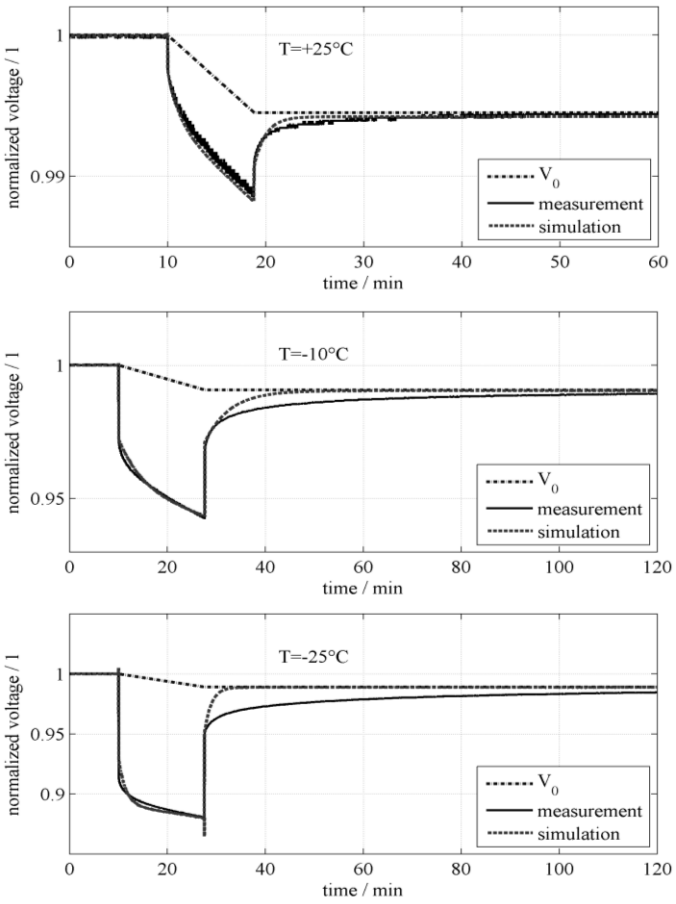

Figure 12: Voltage responses to C/3 current pulse at different temperatures

a more symmetrical distribution. Evaluation of the average voltage deviation (cf. Table 2) confirms this visual impression. To further analyze the source of error, two cycle simulations at different temperatures shall be compared. Figure 15 and Figure 16 show a comparison of a power-based simulation and the corresponding measurement of the battery's clamp voltage at the first thousand seconds of driving in the FTP-72 cycle. Note that for better visibility the voltage axis of the +23°C measurement has been zoomed to display the same amplitude. As already mentioned, the relative error of the voltage response compared to the amplitude seems to be similar at the two selected temperatures.

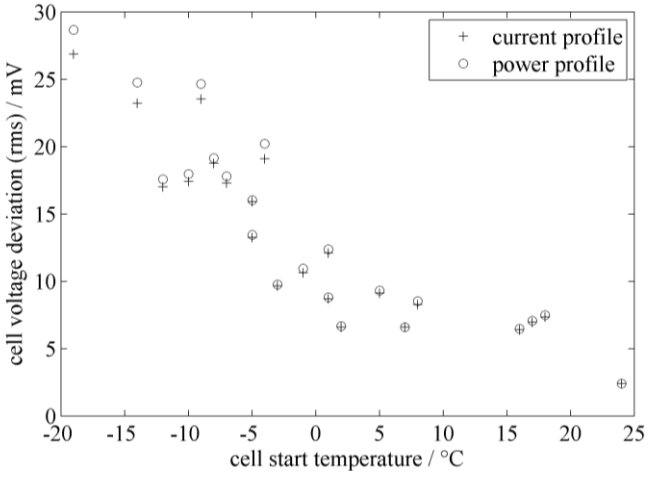

Figure 13: Cell voltage model deviation throughout one FTP-72 cycle using current and power-based load profile

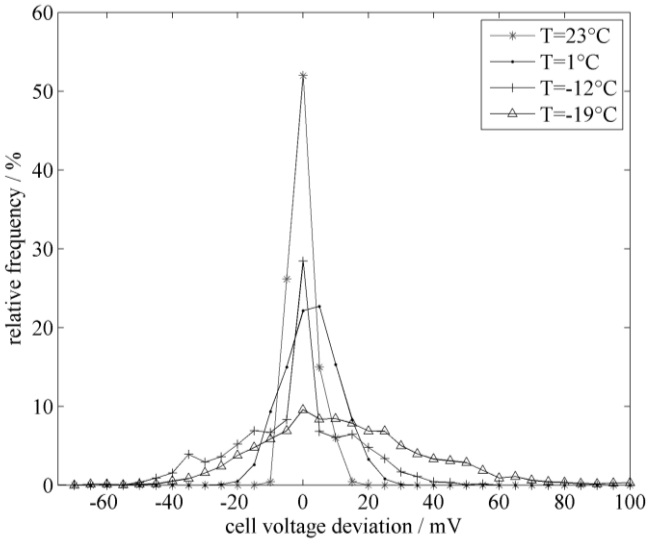

Figure 14: Histogram of cell voltage model deviation throughout one FTP-72 cycle using power-based load profile

Table 2: Statistic analysis of voltage model deviation throughout one FTP-72 cycle using power-based load profile

Cell voltage deviation /mV	**T=23°C**	**T=1°C**	**T=-12°C**	**T=-19°C**
Average	0.12	2.60	-2.55	11.96
σ	3.89	8.41	17.38	26.06
rms	3.89	8.8	17.57	28.66
95th percentile	8.37	16.92	25.17	55.86
99th percentile	10.13	20.61	32.70	69.99

During peaks the voltage is represented equally well by the simulation. The constant voltage level during standstill, however, shows different simulation quality throughout the cycle measurement. Since the power demand during these phases is approximately identical, the deviation in the model has to be caused by the time-dependent part. At +23°C this is the case at point 4 whereas in the -19°C measurement it takes until phase 9 for the error to go back. Considering that the time constant of the RC-couple is five times higher at -19°C it is very likely that the temporary deviation is caused by the time-dependent reactions that are not modeled correctly during the phase of high power. The numbers in Figure 15 and Figure 16 mark the phases of vehicle standstill. Between phase 2 and 3 the cycle has the highest velocity of up to ninety km/h (cf. Figure 3), thus drawing the most power from the battery.

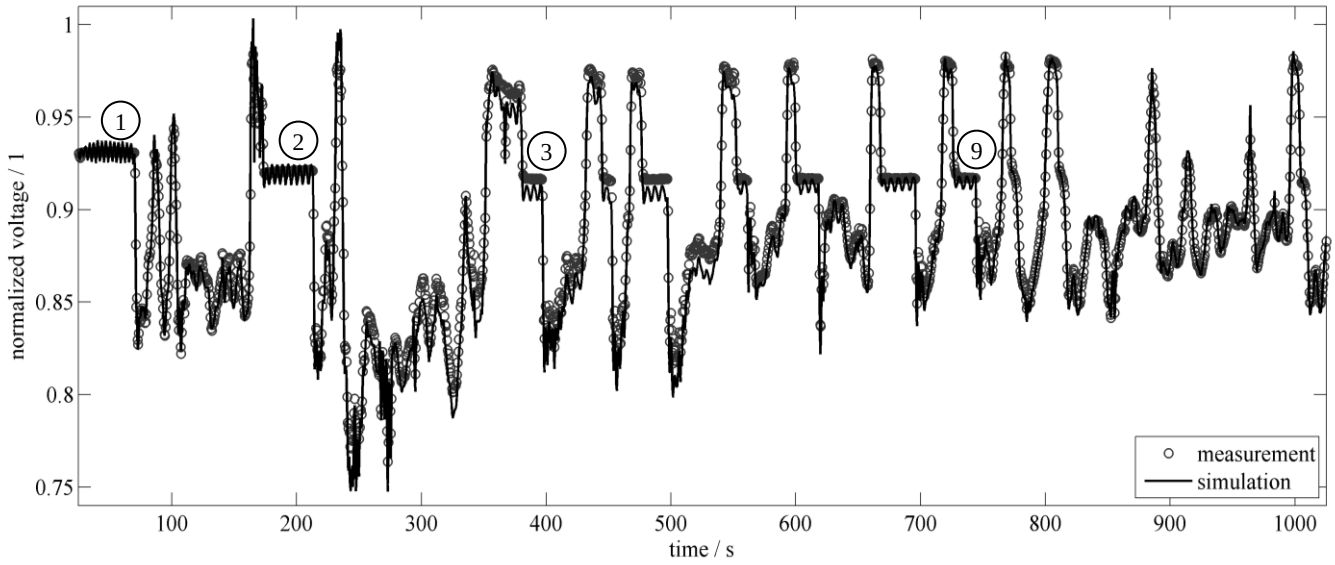

Figure 15: Clamp voltage progression during FTP-72 cycle at -19°C

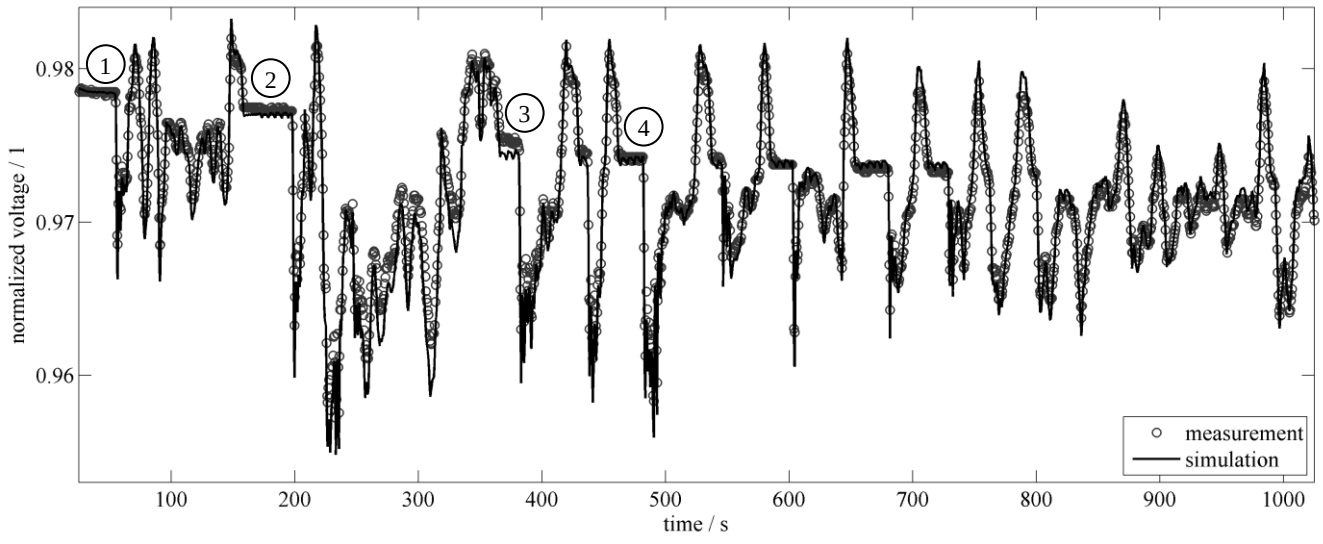

Figure 16: Clamp voltage progression during FTP-72 cycle at +23°

Right after this high power phase, the voltage seems to have drifted, as clearly visible in phase 2. After a certain time the voltage error accumulated during 2 and 3 disappears again. The simulation quality between phase 2 and 3 could not be improved by modifying the R_S parameter without big sacrifices of accuracy in other phases. An evaluation of the zero crossings of the clamp current as described in chapter 3.4 rather indicated that the voltage drop over the RC-couple is too high in the course of the high power phase. Throughout the rest of the drive cycle, mainly representing stop-and-go inner city traffic, the simulation quality is better. Therefore, the approach of using only one current value to parameterize the time-dependent behavior, i.e. the RC-couple, seems not to be applicable for mixed drive cycles that include constant high power phases as well as inner city traffic. At least one more current value should be used during parameterization to account for the different behavior at high average power. The poor fitting quality during relaxation visible in Figure 12, however, did not seem to influence the simulation quality. As already mentioned, the drive cycle measurements also do not include any relaxation phases, only variations of electric power demand.

5 CONCLUSIONS

- As this work illustrates, the energy conversion efficiency of a lithium ion battery is equivalent to the voltage drop during operation. It is also directly linked to the performance of the battery, making it a key system state variable. Since relevant battery parameters like the idle voltage cannot be directly measured, the development of a battery model is necessary for online efficiency estimation as well as for offline simulations. The challenge of this task lies in the nonlinearity of the battery behavior and the distinct dependency on cell temperature.
- Selected vehicle- as well as cell-based measurements were shown to demonstrate the phenomenological effect of low temperatures on the battery behavior. This motivated the development of a battery model that incorporates individual temperature dependency for all model components.
- An equivalent circuit battery model was developed that showed similar simulation quality on a temperature scale from -20°C to +24°C. The results indicated that the quality could be further increased during phases of higher power demand by using additional current values during the parameterization process. For the inner city part of the FTP-72 cycle the model showed acceptable accuracy using only one RC-couple parameterized at one current level.
- A pragmatic approach was presented to parameterize the battery model incrementally which allowed the use of various measurement sources and fitting methods. In this work only graphic parameterization was used but the approach can also be applied for other types of parameter fitting. The key of this approach was to regard the battery behavior as a superposition of instantaneous (time-independent) behavior and delayed (time-dependent) reactions. Using current-based profiles the different reactions do not depend on each other and can be parameterized incrementally. Additionally, this approach allows the validation of intermediate simulation results. Applying these methods allowed narrowing down the source of the voltage deviation during the high power phase of the FTP-72 cycle to the RC-couple.
- The result of the parameterization process showed a distinct dependence of the parameters on temperature. The modeled serial resistance showed *Butler-Volmer* characteristic which explained the battery behavior observed in FTP-72 drive cycle measurements at various temperatures. The time constant of the RC-couple showed almost linear increase at lower temperatures. The high variation of the model parameters over temperature shows that this degree of freedom cannot be neglected to achieve good simulation results at low temperatures.

6 ACKNOWLEDGEMENT

This work is supported in part by the German Bundesministerium für Bildung und Forschung (Federal Ministry of Education and Research) as part of the research project EFA2014/2 (Energy Efficient Driving 2014 – phase 2) [15].

7 REFERENCES

[1] F. Kessler, E. Hockgeiger, J. Schroeder, D. Strobl, J. Tachtler, and F. Vogel, "The new BMW electric powertrain in the ActiveE," *20th Aachen Colloquium Automobile and Engine Technology*, 2011.

[2] C. Gould, J. Wang, D. Stone, and M. Foster, "EV / HEV Li-ion Battery Modelling and State- of-Function Determination," *Interantional Symposium on Power Electronics, Electrical Drives, Automation and Motion*, pp. 353–358, 2012.

[3] H. Zhang and M.-Y. Chow, "Comprehensive Dynamic Battery Modeling for PHEV Applications," *IEEE Power and Energy Society General Meeting*, pp. 1–6, 2010.

[4] M. A. Roscher, "Zustandserkennung von LiFePo-Batterien für Hybrid- und Elektrofahrzeuge," *Dissertation Rheinisch-Westfälische Technische Hochschule Aachen*, 2010.

[5] S. Buller, *Impedance-Based Simulation Models for Energy Storage Devices in Advanced Automotive Power Systems*. 2002.

[6] G. L. Plett, "Results of Temperature-Dependent LiPB Cell Modeling for HEV SOC Estimation," in *Electric Vehicle Symposium*, 2005, no. 1, pp. 1–9.

[7] B. Schweighofer, H. Wegleiter, M. Recheis, and P. Fulmek, "Fast and accurate battery model applicable for EV and HEV simulation," *IEEE International Instrumentation and Measurement Technology Conference Proceedings*, pp. 565–570, May 2012.

[8] J. Hafsaoui, J. Scordia, F. Sellier, and P. Aubret, "Development of an Electrochemical Battery Model and Its Parameters Identification Tool," *International Journal of Automotive Engineering*, vol. 3, pp. 27–33, 2012.

[9] D. M. Bernardi and J.-Y. Go, "Analysis of pulse and relaxation behavior in lithium-ion batteries," *Journal of Power Sources*, vol. 196, no. 1, pp. 412–427, Jan. 2011.

[10] W. Dreyer, J. Jamnik, C. Guhlke, R. Huth, J. Moskon, and M. Gaberscek, "The thermodynamic origin of hysteresis in insertion batteries.," *Nature materials*, vol. 9, no. 5, pp. 448–53, May 2010.

[11] X. G. Yang and B. Y. Liaw, "In situ electrochemical investigations of the kinetic and thermodynamic properties of nickel ± metal hydride traction batteries," vol. 102, 2001.

[12] V. Wang, C. Y.Srinivasan, "Computational battery dynamics (CBD)— electrochemical / thermal coupled modeling and multi-scale modeling," *Journal of Power Sources*, vol. 110, pp. 364–376, 2002.

[13] K. J. Laidler, "A glossary of terms used in chemical kinetics, including reaction dynamics," *Pure and Applied Chemistry*, vol. 68, pp. 149–192, 1996.

[14] L. Song and J. W. Evans, "Electrochemical-Thermal Model of Lithium Polymer Batteries," vol. 147, no. 6, pp. 2086–2095, 2000.

[15] R. Huber and T. Knoll, "Presse-Information der Projektpartner im Forschungsprojekt „Energieeffizientes Fahren 2014 – Reichweitenerhöhung von Elektrofahrzeugen" (EFA 2014/2)," *Press release*, 2012. [Online]. Available: https://www.press.bmwgroup.com. [Accessed: 09-Jan-2013].

[16] ECOpoint Inc, "Worldwide engine and vehicle test cycles." [Online]. Available: http://dieselnet.com/standards/cycles. [Accessed: 07-Feb-2013].

[17] A. Jossen, "Fundamentals of battery dynamics," *Journal of Power Sources, Vol. 154, No. 2*, pp. 530–538, Mar. 2006.

[18] L. W. Juang, P. J. Kollmeyer, T. M. Jahns, and R. D. Lorenz, "Improved nonlinear model for electrode voltage-current relationship for more consistent online battery system identification," *IEEE Energy Conversion Congress and Exposition*, pp. 2628–2634, Sep. 2011.